Planet. Space Sci., Vol. 36, No. 1, pp. 47–53, 1988
Printed in Great Britain.

0032–0633/88 $3.00+0.00

THE PRODUCTION OF O(^{1}D) FROM DISSOCIATIVE RECOMBINATION OF O_2^+*

STEVEN L. GUBERMAN
Institute for Scientific Research, 33 Bedford St., Lexington, MA 02173, U.S.A.† and
Harvard-Smithsonian Center for Astrophysics, 60 Garden St., Cambridge, MA 02138, U.S.A.

(*Received* 27 *July* 1987)

Abstract—The results of large scale *ab initio* calculations of the rates for production of O(^{1}D) by dissociative recombination of O_2^+ are presented for electron temperatures in the range 100–3000 K. A $^1\Delta_u$ state is the dominant dissociative route from $v = 0$ and a $^3\Sigma_u^-$ state is the most important route from $v = 1$ and $v = 2$. The calculated total rate for O(^{1}D) production from $v = 0$ is $2.21(+0.21, -0.24) \times 10^{-7} \times (T_e/300)^{-0.46}$ near room temperature. The $v = 1$ and $v = 2$ rates are about 17% and 47% smaller, respectively, than the $v = 0$ rate at 300 K.

1. INTRODUCTION

For the molecular ion, AB^+, dissociative recombination (DR) with an electron is described by

$$AB^+ + e^- \rightarrow A + B \qquad (1)$$

where A or B are ground or excited state atoms or molecular fragments. The study of the process of DR of molecular ions with electrons began with the suggestion of Bates and Massey (1947) that DR could be an important sink for electrons in the ionosphere. It is now recognized that DR can be a rapid process in a wide variety of plasma environments.

Alex Dalgarno has made many significant contributions to the study of DR. These have ranged from fundamental studies of the DR mechanism to applications in interstellar and atmospheric chemistry. The interstellar studies (Dalgarno, 1976, 1982, 1983, 1985, 1986; Dalgarno *et al.*, 1973; Black and Dalgarno, 1977; Dalgarno and Black, 1976) have explored the DR of a wide variety of molecules, ranging in size from H_2^+ to $C_2H_5OH_2^+$. Several of the atmospheric studies of DR (Dalgarno, 1958, 1983) have focused on the role of DR in the production of the red line of atomic O (Dalgarno, 1958; Dalgarno and Walker, 1964; Abreu *et al.*, 1986). Additional contributions relevant to the theory of DR have encompassed the calculation of the energies (Dalgarno and Drake, 1971) and widths (Bransden and Dalgarno, 1952, 1953a, b) of autoionizing states and the definition of diabatic states (Dalgarno, 1980). An analysis of the mechanism of DR (Bates and Dalgarno, 1962), based upon the earlier work of Bates (1950a, b), provided a number of important insights into DR. Perhaps most relevant to the work presented below was the prediction that the electron temperature dependence of the DR rate coefficient is $T_e^{-0.5}$ unless the curve crossing of the dissociative and molecular ion states leads to a rapid variation of the Franck–Condon factors with electron energy.

One of the examples presented by Bates and Dalgarno (1962) was the DR of O_2^+ with an electron, $O_2^+ + e^- \rightarrow O + O$. It is now well recognized that DR of O_2^+ is an important source of O(^{1}D) in the aurora (Dalgarno and Reid, 1969; Bates, 1982; Rees and Roble, 1986) and airglow (Schaeffer *et al.*, 1972; Bates, 1982; Sharp, 1986).

This paper reports the first large scale *ab initio* calculations of the rate coefficient for generation of O(^{1}D) atoms from DR from O_2^+ in one of the lowest three vibrational levels. The next section has a discussion of the techniques used to accurately determine the potential curves for the important dissociative routes of O_2. The method used for calculating the cross-sections and rates is discussed in Section 3. The approach used for determining autoionization widths is summarized in Section 4 and the resulting rates for O(^{1}D) production are presented in Section 5.

2. POTENTIAL CURVES

In a seminal paper, Bates (1950b) pointed out that DR rates of significant magnitude at low electron energies require that a repulsive potential curve, describing the motion of the products in (1), crosses the ion curve within the turning points of the ion vibrational level undergoing recombination. Since the

* Dedicated to ALEX DALGARNO in his sixtieth year in honour of his many important contributions to aeronomy.
† Current address.

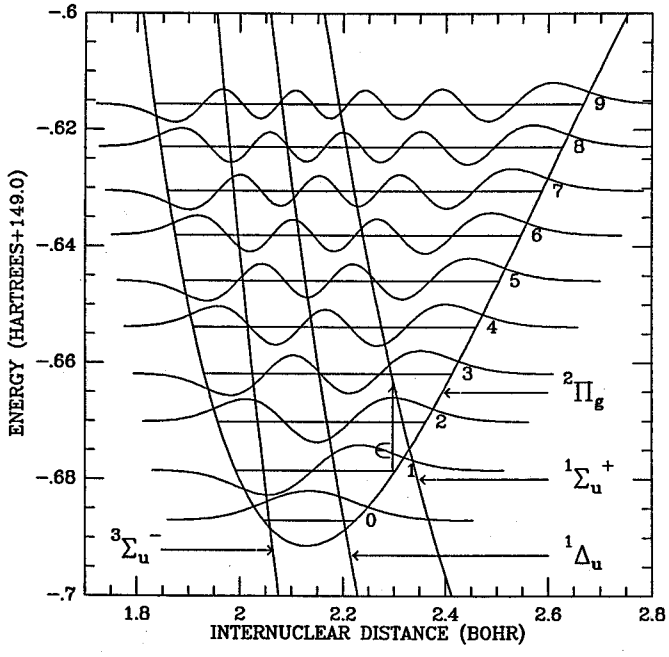

FIG. 1. POTENTIAL ENERGY CURVES FOR DR LEADING TO O(^{1}D).
The three important calculated repulsive routes for DR of the lowest three vibrational levels are shown. The bound potential for the ion is taken from Krupenie (1972) and calculated points (Guberman, 1988b). The vibrational wave functions are each plotted on the same scale and are obtained from the numerical solution of the nuclear Schroedinger equation.

time for dissociation can often be rapid compared to the time for emission of the captured electron, the rate of DR can indeed be fast. The process is illustrated in Fig. 1 where an ion in the $v = 1$ vibrational level undergoes DR by capture of an electron of energy ε. For the DR of O_2^+, inspection of the relevant potential curves (Guberman, 1983) shows that for the lowest three vibrational levels of the ion, only five repulsive states can yield O(^{1}D). The states of interest are the lowest states of $^3\Sigma_u^-$, $^1\Delta_u$, $^1\Sigma_u^+$, $^1\Pi_g$ and $^3\Pi_g$ symmetries. The latter two states do not dissociate adiabatically to ^{1}D atoms but have avoided crossings with higher states that lead to ^{1}D atoms. However, the two Π states have exceedingly small calculated widths, 0.0030 eV for $^1\Pi_g$ and 0.0022 eV for $^3\Pi_g$ (Guberman, 1988a) at $R = 2.2819\ a_0$. These widths are about two orders of magnitude smaller than the smallest width calculated (see Section 4) for the other three states. Since these small widths will lead to very small DR rates, these states are neglected in the calculation of the total DR rate for production of ^{1}D atoms. The calculated potential curves for the remaining three states are shown in Fig. 1. The potential curves have been calculated using contracted Gaussian basis sets of [6s, 3p, 2d, 1f] size. The basis sets have been chosen to exclude Rydberg character and the resulting potential curves describe the diabatic valence states needed for DR. The orbitals are determined separately for each state in Complete Active Space Self-Consistent Field (CASSCF) calculations (Roos *et al.*, 1980) and the Configuration Interaction (CI) wave functions are generated by taking all single and double excitations from a multireference set of configurations to the full virtual orbital space. The direct CI method (Siegbahn, 1980) and the MOLECULE (Almlof)–SWEDEN (Siegbahn *et al.*) programs were used for the calculation of the potential curves. The CI energies have been corrected for the missing quadruple excitations (Langhoff and Davidson, 1974). The final CI wave functions for the $^3\Sigma_u^-$, $^1\Delta_u$ and $^1\Sigma_u^+$ states had 228,036, 185,400 and 139,946 terms, respectively. Further details of the calculations will be reported separately (Guberman, 1988b).

The $^3\Sigma_u^-$ state shown in Fig. 1 intersects the ion at the small R turning point of the $v = 0$ level and is the diabatic continuation of the repulsive wall of the upper state of the well-known Schumann–Runge bands. Dissociation along $^3\Sigma_u^-$ after capture by a zero energy electron from $v = 0$ leads to a ground-state atom and a ^{1}D atom, each with 2.5 eV kinetic energy.

Dissociation along the $^1\Delta_u$ route from $v = 0$ leads to two ^{1}D atoms, each with 1.5 eV kinetic energy. Dissociation along $^1\Sigma_u^+$ leads to a ^{1}S and a ^{1}D atom, each with 0.4 eV kinetic energy from $v = 0$.

3. METHODS FOR CROSS-SECTIONS AND RATES

The cross-sections, σ_v, for direct DR (Bardsley, 1968a) from ion vibrational level v have been calculated using the expression derived by Giusti (1980) from quantum defect theory for the case of a single dissociative state and many open ion vibrational levels, v',

$$\sigma_v = (\pi r/2k_e^2)[4\xi_v/(1+\Sigma_{v'}\xi_{v'})^2] \quad (2)$$

where $k_e^2 = 2m\varepsilon$, k_e is the wave number of the incident electron, m is the electron mass, and r the ratio of multiplicities of the neutral and ion states. The matrix elements ξ_v are given by

$$\xi_v = (\pi/2)[\langle X_v|\Gamma^{1/2}(R)|X_d\rangle]^2 \quad (3)$$

where X_v and X_d are vibrational wave functions for the ion and dissociative states, respectively. The integration in (3) is over both R and the electronic coordinates. The vibrational wave functions are determined by the Numerov method on a $0.001\,a_0$ grid between 0.0 and $8.0\,a_0$. The integration over R in (3) is done by the rectangular rule. The width, $\Gamma(R)$, connects the electronic continuum of the free electron and ion to the repulsive dissociating resonance state and is given by the Golden Rule,

$$\Gamma(R) = 2\pi\langle\{\Phi_{ion}(x,R)\phi_\varepsilon(x,R)\}|H|\Phi_d(x,R)\rangle^2. \quad (4)$$

In (4) H is the Hamiltonian, the integration is over the electronic coordinates represented by x, and the wave functions from left to right in (4) are for the ion core, the free electron, and the dissociative neutral state. The antisymmetrized product of the ion core and free electron wave functions is denoted by $\{\ \}$.

The indirect DR process (Bardsley, 1968b; Giusti, 1980; Giusti-Suzor *et al.*, 1983) in which recombination occurs into a vibrationally excited Rydberg state which is predissociated by the repulsive routes discussed here, has not been included in the cross-section calculations. The indirect process is not expected to be a significant contributor to O(^{1}D) production. Rate constants have been calculated by averaging the calculated cross-sections over a Maxwellian distribution of electron energies.

4. ELECTRONIC WIDTHS

The widths given in equation (4) have been calculated by using high Rydberg orbitals to represent the free electron (Guberman, 1986, 1988a). Since all the orbital amplitudes in (4), except for that of the free electron, fall off rapidly with increasing x, only the free electron amplitude near the nuclei is needed for the width calculation. Except for a normalization factor, high Rydberg orbitals have a shape similar to free electron orbitals near the nuclei. A density of states is then inserted into (4) for the normalization (Guberman, 1988a). The Rydberg orbitals are calculated using the Improved Virtual Orbital (IVO) method (Hunt and Goddard, 1969) in a basis set of 18 diffuse Gaussians positioned midway between the nuclei (Guberman, 1988a). Each Rydberg orbital is an eigenfunction of an IVO Hamiltonian which is unique for each molecular symmetry.

The wave function of the ion plus a free electron in (4) is represented by antisymmetrized products of a valence CI description of the ground state of O_2^+ with the Rydberg orbital and with the valence virtual orbitals of the same symmetry as the Rydberg orbital. For the width calculations, the dissociative states were represented by full valence CI wave functions in which excitations out of the 2σ orbitals were included. For $^3\Sigma_u^-$ this procedure leads to a 48 term CI wave function for the dissociative state and a 954 term CI wave function for the entrance channel. For $^1\Delta_u$ and $^1\Sigma_u^+$, the entrance and exit channel wave functions have 42 and 630 terms, respectively. The size of the entrance channel wave function is increased further by allowing the entrance channel to mix in higher nonphysical routes from the exit channel. A Feshbach (1958) projection operator procedure has been used to implement this procedure (Guberman, 1986, 1988a).

The entire procedure is repeated for several values of the Rydberg orbital principal quantum number with the highest accurately determined orbital having $n = 8$. The widths calculated from each value of n are then extrapolated to the continuum. A comparison to experimentally derived (Galluser and Dressler, 1982) predissociation matrix elements for NO indicates that the widths calculated by this procedure deviate from experiment by about 15%.

For $^3\Sigma_u^-$, the calculated width is 0.81 eV near $R = 2.08\,a_0$ and decreases to 0.54 eV at $1.78\,a_0$. For $^1\Delta_u$ and $^1\Sigma_u^+$, the width is relatively constant with R, having a value of 0.44 and 0.29 eV, respectively, at $R = 2.28\,a_0$, varying by only about 2% over the region of significant nuclear overlap with the $v = 0, 1, 2$ ion wave functions. Since the estimated uncertainty in the calculated widths is 15%, the variation of the width with R has been ignored for $^1\Delta_u$ and $^1\Sigma_u^+$ but has been accounted for in expression (3) for $^3\Sigma_u^-$ (Guberman, 1988b).

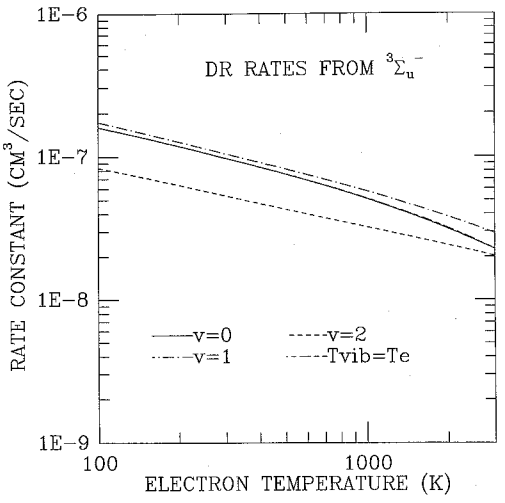

FIG. 2. CALCULATED DR RATES ALONG THE $^3\Sigma_u^-$ DISSOCIATIVE ROUTE LEADING TO $O(^3P)+O(^1D)$ FROM THE LOWEST THREE VIBRATIONAL LEVELS OF THE ION.
Also shown is the rate for the case in which the vibrational temperature is the same as the electron temperature. The rates are for non-rotating molecules.

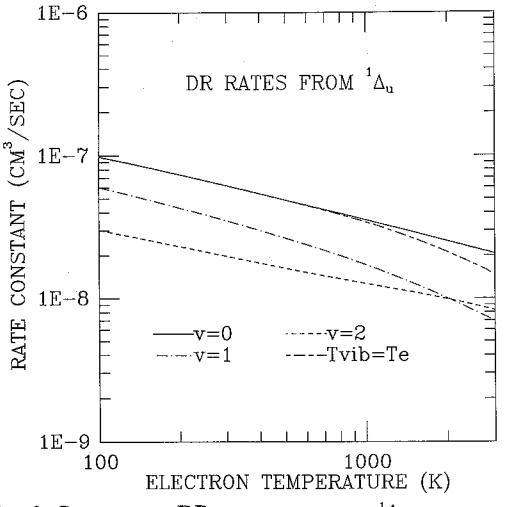

FIG. 3. CALCULATED DR RATES ALONG THE $^1\Delta_u$ DISSOCIATIVE ROUTE LEADING TO $O(^1D)+O(^1D)$ FROM THE LOWEST THREE VIBRATIONAL LEVELS OF THE ION.
Also shown is the rate for the case in which the vibrational temperature is the same as the electron temperature. The rates are for non-rotating molecules.

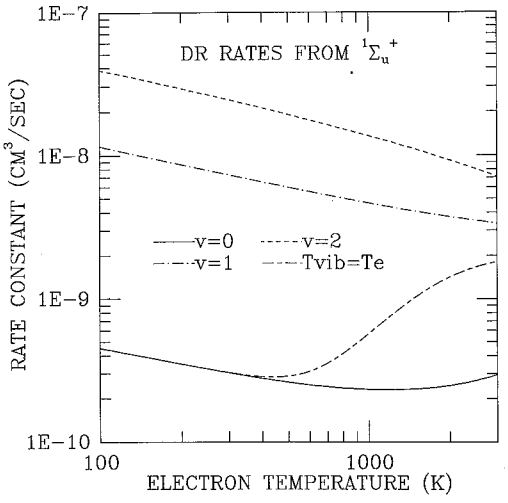

FIG. 4. CALCULATED DR RATES ALONG THE $^1\Sigma_u^+$ DISSOCIATIVE ROUTE LEADING TO $O(^1S)+O(^1D)$ FROM THE LOWEST THREE VIBRATIONAL LEVELS OF THE ION.
Also shown is the rate for the case in which the vibrational temperature is the same as the electron temperature. The rates are for non-rotating molecules.

5. CALCULATED DR RATES

The calculated rate constants for the three dissociative routes discussed here are shown in Figs 2, 3 and 4 for each of the lowest three vibrational levels of the nonrotating ion. For $200 \leqslant T_e \leqslant 400$ K, the DR rates are given in Table 1. The uncertainties in the rates are average uncertainties computed from an estimated $\pm 15\%$ uncertainty in the calculated widths and an estimated ± 0.1 eV uncertainty in the position of the potential curves relative to the ion curve. The highest DR rates are from $^3\Sigma_u^-$. However, for $v = 0$, the rate along $^1\Delta_u$ is more than half the DR rate along $^3\Sigma_u^-$. Since $^1\Delta_u$ leads to two ^{1}D atoms, the highest rates for producing ^{1}D atoms for $v = 0$ are from $^1\Delta_u$. However, from $v = 1$ and $v = 2$ (Figs 2–4), the highest rates for $O(^1D)$ production are from $^3\Sigma_u^-$.

As pointed out by Bates and Dalgarno (1962), the temperature dependence of the direct DR process will vary as $T_e^{-0.5}$ if the amplitude of the ion wave function does not vary substantially over the range of electron energies of interest. Such a situation can arise for any ion wave function if the dissociative curve is very steep. In general, an intersection of the dissociative route with the ion vibrational level near the peak of the ion wave function will lead to slowly varying nuclear overlap terms and electron temperature dependencies near -0.5, while intersection at a point where the absolute value of the ion wave function amplitude is increasing (decreasing) will usually lead to temperature dependencies more positive (negative) than -0.5. Note that the denominator in (2) has a tempering effect upon these conclusions. Two such cases are illustrated in Cases (a) and (b) of Fig. 2 of Bates and Dalgarno (1962). The latter case shows a dissociative route intersecting the $v = 0$ level in the nonclassical region on the large R side of the ion equilibrium internuclear distance and resembles the situation found here for $^1\Sigma_u^+$.

TABLE 1. DISSOCIATIVE RECOMBINATION RATES ALONG THREE CHANNELS FOR EACH OF THE LOWEST THREE VIBRATIONAL LEVELS OF THE ION AT 200 K $\leqslant T_e \leqslant$ 400 K AND $J = 0$*

v	$^3\Sigma_u^-$	$^1\Delta_u$	$^1\Sigma_u^+$	Total ^{1}D production rate
0	0.97(+0.09, −0.10)[0.48]	0.62(+0.06, −0.07)[0.45]	0.0030(+0.0016, −0.0011)[0.34]	2.21(+0.21, −0.24)[0.46]
1	1.05(+0.05, −0.07)[0.47]	0.35(+0.06, −0.07)[0.52]	0.073(+0.019, −0.017)[0.41]	1.82(+0.19, −0.23)[0.49]
2	0.53(+0.06, −0.08)[0.42]	0.20(+0.05, −0.06)[0.39]	0.24(+0.03, −0.04)[0.45]	1.17(+0.19, −0.24)[0.42]

* All rates are total recombination rates except for the last column which is the rate for production of ^{1}D atoms. The rates in the last column are obtained by adding columns 2 and 4 to twice column 3. The electron temperature dependence is shown in square brackets following each rate. Each rate is multiplied by 10^{+7}. The rate for $^3\Sigma_u^-$ from $v = 0$ is read as $0.97(+0.09, -0.10) \times 10^{-7} \times (T_e/300)^{-0.48}$.

For $^1\Sigma_u^+$, the amplitudes of the ion wave functions at low electron energies increase most rapidly for $v = 0$. The increase for $v = 1$ is less rapid than for $v = 0$. For $v = 2$, the intersection is near the outer peak in the $v = 2$ wave function. The calculated temperature dependencies given in Table 1 for $^1\Sigma_u^+$ show the predicted pattern. The most positive exponent is for $v = 0$ followed by $v = 1$ and $v = 2$. For the other two dissociative routes the exponents are near 0.5 for $v = 0$ since the intersections with the ion are within the classical turning points and the amplitude is changing slowly. For $v = 1$ and 2 and $^3\Sigma_u^-$ and $^1\Delta_u$, one must take into account the overlap of the nodes in the ion wave functions with the nodes in the continuum wave functions. The exponents are difficult to predict in these cases by visual inspection of Fig. 1.

Also shown in Figs 2–4 are the rates for the equilibrium case where the vibrational temperature is set equal to the electron temperature. For $^3\Sigma_u^-$, the equilibrium case rates are nearly indistinguishable from the $v = 0$ rates over the span of electron temperatures plotted. For $^1\Delta_u$, the equilibrium rates fall below the $v = 0$ rates at high electron temperatures. For $^1\Sigma_u^+$, the equilibrium rates increase dramatically above 450 K, since the rates for $v = 1$ and $v = 2$ are substantially larger than for $v = 0$ (Guberman, 1987).

It is interesting to examine the ^{1}D production in each channel as a function of ion vibrational level. From $v = 0$, 56% of the ^{1}D atoms arise from the $^1\Delta_u$ channel and 44% arise from the $^3\Sigma_u^-$ channel. For $v = 1$, 58% of the ^{1}D atoms are in the $^3\Sigma_u^-$ channel and 4% appear in the $^1\Sigma_u^+$ channel with 0.52 eV kinetic energy. For $v = 2$, 45% of the atoms are in the 2.7 eV $^3\Sigma_u^-$ channel and 21% are in the 0.64 eV $^1\Sigma_u^+$ channel. Each vibrational level will lead to a unique three component Doppler line shape. From these data, the vibrational distribution of the recombining ion could be determined in an experiment that accurately determines the Doppler widths of the radiating ^{1}D atoms.

The total rate for producing ^{1}D atoms for T_e in the above range from $v = 0$ (Table 1) is

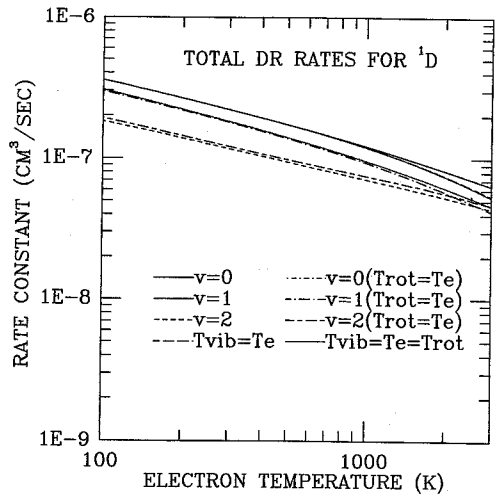

FIG. 5. CALCULATED TOTAL DR RATES FOR PRODUCTION OF O(^{1}D) FROM THE LOWEST THREE VIBRATIONAL LEVELS OF THE ION.
Both the $J = 0$ rates and rates for which the rotational temperature is the same as the electron temperature are shown.

$$2.21(+0.21, -0.24) \times 10^{-7} \times (T_e/300)^{-0.46}\,\mathrm{cm^3\,s^{-1}}$$

and is in good agreement with the value originally reported by Zipf (1970) of $1.9 \times 10^{-7}\,\mathrm{cm^3\,s^{-1}}$. Note that the total calculated rate decreases with increasing v. The rate from $v = 2$ is about half the rate from $v = 0$. The variation of the rate with v contrasts sharply to that for producing O(^{1}S) (Guberman, 1987) shown in the fourth column of Table 1 and Fig. 4. The rotationless O(^{1}S) rate for $v = 2$ is a factor of 80 larger than the rate from $v = 0$. The total calculated rate up to $T_e = 3000$ K for ^{1}D production is shown in Fig. 5. Rates for both $J = 0$ and rotationally averaged rates in which the rotational temperature is the same as T_e are shown. Clearly, accounting for the rotational temperature has only a slight effect upon the calculated rates. The rotationally averaged and the rotationless results from $v = 0$ and for the case

of equal vibrational and electron temperatures are each superimposed on the scale of Fig. 5.

There have been several aeronomic determinations of the ^1D production rate by DR. The literature prior to 1982 has been reviewed by Torr and Torr (1982). Among the deduced production rates are $(2.1 \pm 0.48) \times 10^{-7} \times (T_e/300)^{-0.55}$ (Hays *et al.*, 1978; Link *et al.*, 1981) and $(1.96 \pm 0.67) \times 10^{-7} \times (T_e/300)^{-0.55}$ (Abreu *et al.*, 1983). These rates were obtained by combining the total rate found by Walls and Dunn (1974) and Torr *et al.* (1976) with a model determination of the ^1D quantum yield. A recent determination (Abreu *et al.*, 1986) which improves the models by including quenching of $O(^1D)$ by $O(^3P)$ leads to a rate of $1.9 \times 10^{-7} \times (T_e/300)^{-0.55}$. The deduced rates are in excellent agreement with the $v = 0$ rate calculated here at room temperature. The atmospheric quantum yields are derived at ionospheric temperatures. At $T_e = 760$ K, the ^1D production rate calculated here is $1.41(+0.14, -0.16) \times 10^{-7}$ compared to the model rate (Abreu *et al.*, 1986) of 1.14×10^{-7}. Considering the likely precision on the latter rate, the rates reported here are in agreement with the model rates. Note that the precision on the rates calculated here do not exclude the possibility that the models apply to vibrationally excited O_2^+.

None of the above models have included ^1D production due to cascade from ^1S. The DR contribution to cascade will be unimportant if the ion is mostly in $v = 0$ but should be considered if a substantial fraction of the ions are vibrationally excited.

6. CONCLUSIONS

Three neutral dissociative states of $^3\Sigma_u^-$, $^1\Delta_u$ and $^1\Sigma_u^+$ symmetries have been identified as the major sources of $O(^1D)$ from DR of the lowest three vibrational levels of O_2^+. DR rates along each of these routes have been calculated for electron temperatures in the range 100–3000 K. The total rate for generating DR from $v = 0$,

$$2.21(+0.21, -0.24) \times 10^{-7} \times (T_e/300)^{-0.46} \text{ cm}^3 \text{ s}^{-1},$$

agrees with prior rates determined from aeronomic models and laboratory measurements. However, the variation of the rate with v and the precision on the calculated rates leaves room for the possibility that the atmospheric models and the laboratory experiments could be observing vibrationally excited ions. The total rate for generating $O(^1D)$ decreases with increasing v in contrast to the rates for generating $O(^1S)$ which increase markedly with increasing v.

Acknowledgements—This research was supported at ISR by Nasa Ames Cooperative Agreement NCC 2-308, by the National Science Foundation under grant ATM-8616776, and by the National Center for Atmospheric Research which is sponsored by the National Science Foundation. Support at CFA was provided by the Air Force Office of Scientific Research under grant AFOSR-84-0109.

REFERENCES

Abreu, V. J., Solomon, S. C., Sharp, W. E. and Hays, P. B. (1983) The dissociative recombination of O_2^+: the quantum yield of $O(^1S)$ and $O(^1D)$. *J. geophys. Res.* **88**, 4140.

Abreu, V. J., Yee, J. H., Solomon, S. C. and Dalgarno, A. (1986) The quenching rate of $O(^1D)$ by $O(^3P)$. *Planet. Space Sci.* **34**, 1143.

Almlof, J. MOLECULE, a Gaussian integral program.

Bardsley, J. N. (1968a) Configuration interaction in the continuum states of molecules. *J. Phys. B* **1**, 349.

Bardsley, J. N. (1968b) The theory of dissociative recombination. *J. Phys. B* **1**, 365.

Bates, D. R. (1950a) Electron recombination in helium. *Phys. Rev.* **77**, 718.

Bates, D. R. (1950b) Dissociative recombination. *Phys. Rev.* **78**, 492.

Bates, D. R. (1982) Airglow and auroras, in *Applied Atomic Collision Physics* (Edited by Massey, H. S. W. and Bates, D. R.), pp. 149–224. Academic Press, New York.

Bates, D. R. and Dalgarno, A. (1962) Electronic recombination, in *Atomic and Molecular Processes* (Edited by Bates, D. R.), pp. 245–271. Academic Press, New York.

Bates, D. R. and Massey, H. S. W. (1947) The basic reactions in the upper atmosphere II. The theory of recombination in the ionized layers. *Proc. R. Soc.* **192**, 1.

Black, J. H. and Dalgarno, A. (1977) Models of the interstellar clouds. I. The Zeta Ophiuchi cloud. *Astrophys. J. Suppl.* **34**, 405.

Bransden, B. H. and Dalgarno, A. (1952) A variational method for radiationless transitions. *Phys. Rev.* **88**, 148.

Bransden, B. H. and Dalgarno, A. (1953a) The calculation of autoionization probabilities—I. Perturbation methods with application to autoionization in helium. *Proc. Phys. Soc.* **A66**, 904.

Bransden, B. H. and Dalgarno, A. (1953b) The calculation of autoionization probabilities—II. A variational method for radiationless transitions with application to the $(2s)^2$ $^1S-(1sks)^1S$ transition of helium. *Proc. Phys. Soc.* **A66**, 911.

Dalgarno, A. (1958) The altitudes and excitation mechanisms of the night airglow. *Ann. Geophys.* **14**, 241.

Dalgarno, A. (1976) The interstellar molecules CH and CH^+, in *Atomic Processes and Applications* (Edited by Burke, P. G. and Moiseiwitsch, B. L.), pp. 109–132. North-Holland, Amsterdam.

Dalgarno, A. (1980) Diabatic and resonance molecular states. *Physica Scripta* **21**, 492.

Dalgarno, A. (1982) Molecules in interstellar space, in *Applied Atomic Collision Physics* (Edited by Massey, H. S. W. and Bates, D. R.), pp. 427–467. Academic Press, New York.

Dalgarno, A. (1983) Electron–ion and proton–ion collisions in astrophysics, in *Physics of Ion–Ion and Electron–Ion Collisions* (Edited by Brouillard, F. and McGowan, J. W.), pp.1–36. Plenum Press, New York.

Dalgarno, A. (1985) Molecular astrophysics, in *Molecular*